

29 **ABSTRACT**

30 **Background:** Alzheimer's disease neuropathologic changes (AD-NC) are important for
31 identify people with high risk for AD dementia (ADD) and subtyping ADD.

32 **Objective:** Develop imputation models based on clinical measures to infer AD-NC.

33 **Methods:** We used penalized generalized linear regression to train imputation models
34 for four AD-NC traits (amyloid- β , tangles, global AD pathology, and pathologic AD) in
35 Rush Memory and Aging Project decedents, using clinical measures at the last visit
36 prior to death as predictors. We validated these models by inferring AD-NC traits with
37 clinical measures at the last visit prior to death for independent Religious Orders Study
38 (ROS) decedents. We inferred baseline AD-NC traits for all ROS participants at study
39 entry, and then tested if inferred AD-NC traits at study entry predicted incident ADD and
40 postmortem pathologic AD.

41 **Results:** Inferred AD-NC traits at the last visit prior to death were related to postmortem
42 measures with $R^2=(0.188,0.316,0.262)$ respectively for amyloid- β , tangles, and global
43 AD pathology, and prediction Area Under the receiver operating characteristic Curve
44 (AUC) 0.765 for pathologic AD. Inferred baseline levels of all four AD-NC traits
45 predicted ADD. The strongest prediction was obtained by the inferred baseline
46 probabilities of pathologic AD with $AUC=(0.919,0.896)$ for predicting the development of
47 ADD in 3 and 5 years from baseline. The inferred baseline levels of all four AD-NC traits
48 significantly discriminated pathologic AD profiled eight years later with p-
49 values $<1.4 \times 10^{-10}$.

50 **Conclusion:** Inferred AD-NC traits based on clinical measures may provide effective
51 AD biomarkers that can estimate the burden of AD-NC traits in aging adults.

52

53 **KEYWORDS:** Alzheimer's disease; Computational modeling; Alzheimer's disease

54 neurologic change; Dementia; Pathology

55 INTRODUCTION

56 The accumulation of Alzheimer's disease neuropathologic changes (AD-NC),
57 such as amyloid- β and intracellular neurofibrillary tangles, underlying Alzheimer's
58 disease dementia (ADD) has been observed even during the initial stages of ADD when
59 cognition is normal [1]. Higher levels of AD-NC during the early stages of ADD have
60 been shown to be associated with an increased risk of ADD [2-6]. Separate therapies
61 have been developed for targeting the peptide amyloid- β in extracellular amyloid
62 plaques and the protein tau in intracellular neurofibrillary tangles [7-9]. Yet, conventional
63 prediction models identifying adults at risk for clinical ADD do not inform on which AD-
64 NC traits underlie the risk of ADD. Thus, procedures that can accurately infer elevated
65 levels of AD-NC traits in living adults with normal cognition have the potential to
66 facilitate early targeted treatments [10-17].

67 Direct measures of brain AD-NC traits can only be obtained at autopsy. Recent
68 efforts to quantify AD-NC during life have focused on identifying biomarkers of AD-NC
69 traits by using brain imaging or fluid AD biomarkers [18-20]. Recent work comparing tau
70 and amyloid positron emission tomography (PET) brain imaging measures to indices
71 measured at autopsy, suggests that current imaging may not reliably detect the early
72 stages of AD pathology [21, 22]. Particularly, brain imaging and CSF biomarkers are not
73 widely available due to their costs, invasiveness, and difficulty to deploy at scale.
74 Studies focusing on serum biomarkers have advanced rapidly in recent years, yet the
75 field has not converged on specific biomarkers that can be employed in the general
76 population [23-27].

77 Rapid advances in machine learning methods such as penalized generalized
78 linear regression [28] have been employed to impute missing data or infer data that are
79 difficult to be measured directly in biomedical research fields [29-34]. Similarly, the
80 penalized generalized linear regression method could be deployed to develop
81 imputation models based on clinical measures in older adults to infer levels of AD-NC
82 traits. Such imputation models learn the predictive information of postmortem AD-NC
83 traits like tangles from clinical measures obtained prior to death in decedents
84 undergoing autopsy. The imputation model works by mathematically “explaining” the
85 variation of observed AD-NC traits measured in decedents by their equivalence of
86 weighted linear combinations of predictive clinical measures. Once imputation models
87 developed for AD-NC traits are validated in an independent cohort, they can be applied
88 to any older adults with similar clinical measures to infer AD-NC traits.

89 Comprehensive clinical and postmortem data are necessary to develop and
90 validate imputation models for AD-NC traits. This multi-stage study leveraged clinical
91 and postmortem data from two harmonized, independent, longitudinal prospective
92 cohort studies — Rush Memory and Aging Project (MAP) and the Religious Orders
93 Study (ROS) [35]. First, we trained imputation models for four AD-NC traits (amyloid- β ,
94 tangles, global AD pathology, and pathologic AD diagnosis) by applying the penalized
95 generalized linear regression method to clinical measures obtained at the last visit
96 before death and postmortem AD-NC indices measured at autopsy in MAP decedents.
97 Second, we validated the imputation models in a second independent cohort (ROS)
98 which collected the same clinical and postmortem AD-NC traits. Third, we applied the
99 imputation models to clinical measures collected in adults without dementia at study

100 entry to infer baseline levels of AD-NC traits that were on average about eight years
101 before death for decedents (or before last visit for living participants). We demonstrated
102 the efficacy of these interfered baseline AD-NC traits as effective AD biomarkers, by
103 showing their predictivity of future clinical ADD and discrimination of postmortem
104 pathologic AD.

105

106 **MATERIALS AND METHODS**

107 **Participants**

108 Participants were community-dwelling older adults enrolled without known dementia and
109 with at least two annual visits in one of two ongoing longitudinal prospective cohort
110 studies of chronic conditions of aging — MAP (n=1179 with ~500 autopsied) and ROS
111 (n=1103 with ~600 autopsied). Both cohorts employed a harmonized data collection
112 battery administered by the same research assistants facilitating joint analyses. For this
113 study, we included adults without clinical evidence of dementia at enrollment with at
114 least two annual follow-up cognitive assessments. At study entry, 1742 adults had no
115 cognitive impairment (NCI) and 540 adults had mild cognitive impairment (MCI) (**Table**
116 **S1**). The duration of annual follow-up for participants ranged from 2 to 26 years, with an
117 average follow-up of 8 years (SD, 5.42 years) [**Fig S1; Tables S1-S2**].

118

119 **Assessment of AD-NC Traits**

120 After the death of ROS/MAP participants, their brains were removed and
121 hemisected following the standard procedure, as previously described [35]. Tissue

122 blocks were dissected from predetermined regions and used for postmortem diagnosis
123 of pathologic AD. Structured autopsy collected indices of AD/ADRD pathologies that
124 were collected blinded to all prior clinical and cognitive data. This study focuses on the
125 development of imputation models to infer the following four AD-NC traits that were
126 measured in autopsied decedents (**Table S2**).

127 **Amyloid- β** was labeled with an N-terminus-directed monoclonal antibody (10D5;
128 Elan, Dublin, Ireland; 1:1,000). Immunohistochemistry was performed as previously
129 described using diaminobenzidine as the reporter, with 2.5% nickel sulfate to enhance
130 immunoreaction product contrast.

131 **PHFtau (Tangles)** was labeled with an antibody specific for phosphorylated tau
132 (AT8; Innogenetics, San Ramon, CA; 1:1,000). Amyloid- β load and tangles were
133 quantified in 8 brain regions (anterior cingulate cortex, superior frontal cortex, mid
134 frontal cortex, inferior temporal cortex, hippocampus, entorhinal cortex, angular
135 gyrus/supramarginal gyrus, and calcarine cortex). Overall amyloid- β load was calculated
136 through averaging mean percent area of amyloid- β deposition per region, across
137 multiple brain regions. Tangles densities were derived by averaging tangles densities
138 across corresponding brain regions. Measures of amyloid- β and tangles were further
139 square-root transformed to improve their asymptotic normality as previously reported
140 [36, 37].

141 **Global AD Pathology:** A modified Bielschowsky silver stain was used to
142 visualize neuritic plaques, diffuse plaques, and neurofibrillary tangles in five cortical
143 areas (hippocampus, entorhinal, midfrontal, middle temporal, and inferior parietal).
144 Neuritic and diffuse plaques, and neurofibrillary tangles were counted in the region that

145 appeared to have the maximum density of each pathology as previously described. A
146 standardized score was created for each neuropathology in each region by dividing the
147 raw count by the standard deviation of the mean for the same neuropathology in the
148 same region. This standardization procedure puts the pathologic indices on a relatively
149 common scale. A summary global AD pathology score was made based on the average
150 of the greatest density of neuritic plaques, diffuse plaques, and neurofibrillary tangles in
151 one mm² [38, 39]

152 ***Pathologic Diagnosis of AD:*** The National Institute on Aging-Reagan criteria
153 were used with intermediate and high likelihood cases indicating a pathologic diagnosis
154 of AD, which is a binary indicator with value 1 denoting the present of pathologic AD
155 and 0 denoting the absent of pathologic AD [40].

156

157 **Assessment of Composite Cognition Score and Cognitive Status**

158 A structured cognitive assessment was administered annually. The
159 neuropsychological battery included 19 tests that assessed five cognitive abilities
160 (episodic memory, semantic memory, working memory, visuospatial ability/perceptual
161 orientation, and perceptual speed). Raw test scores were standardized for each test
162 using baseline means and standard deviations (SDs) of both cohorts; the resulting Z-
163 scores were then averaged across these cognitive tests to derive a single summary
164 composite cognition score as described in prior publications [35, 41].

165 Cognitive diagnoses were made in a three-step process. Cognitive testing was
166 scored by a computer program and the results were reviewed by a neuropsychologist to
167 diagnose cognitive impairment. Then participants were evaluated by a physician who

168 used available cognitive and clinical data to classify cognitive status at each annual
169 visit. Dementia required meaningful decline in cognitive function with impairment in
170 multiple areas of cognition, and AD required dementia and progressive loss of episodic
171 memory. Individuals with cognitive impairment who did not meet dementia criteria were
172 diagnosed with mild cognitive impairment (MCI). Individuals without dementia or MCI
173 were classified as having no cognitive impairment (NCI). Clinical diagnosis of cognitive
174 status was based on published criteria [42-44]. Participants with dementia due to
175 primary cause other than AD are excluded in this study. At the time of death, select
176 clinical data from the entire study were reviewed by a neurologist, blinded to
177 postmortem data, to render a final cognitive status diagnosis[35].

178

179 **Clinical Covariates**

180 Diverse clinical measures were used to develop imputation models for four AD-
181 NC traits. **Table S3** shows the complete list and groupings of the 57 clinical measures
182 examined in this study, including both cross-sectional and longitudinal variables. Cross-
183 sectional clinical measures were collected only once for each participant, such as sex,
184 education, and *APOE* genotype. Longitudinal clinical measures were collected each
185 time during participants' annual visits. Baseline clinical characteristics are provided in
186 **Tables S2, S4, and S5** and a heat map (**Fig S2**) is included to show the inter-
187 correlations of the clinical variables examined in this study. The measures analyzed in
188 this study were selected after excluding cross-sectional variables with a high proportion
189 of missing values and those that were highly correlated with other selected clinical
190 measures (correlation>0.95). Samples with missing values in the selected cross-

191 sectional clinical measures were excluded. Missing values of longitudinal clinical
192 measures were assumed to be missed at random and were imputed from the measured
193 values at the nearest visit of the same participant, by using the “*fill(.direction = "up")*”
194 function from R library “*tidyr*”. That is, if a participant had a missing value at last visit for
195 a longitudinal variable, the missing value would be imputed as the measured value of
196 this variable in this participant’s nearest previous visit with collected measurement. The
197 percentage of missing data (i.e., missing rate) in the longitudinal clinical measurements
198 at last visit and study baseline were presented in **Fig, S3**. The number of samples that
199 were actually used in the analyses are presented in **Tables S6**, and **S7**.

200

201 **Analytic Approach**

202 A multi-stage analytic approach was employed to develop, validate, and
203 demonstrate the effectiveness of the inferred the levels of four AD-NC traits at study
204 entry as potential AD biomarkers.

205

206 **Developing imputation models to infer AD-NC traits**

207 *Stage 1. Training imputation models.*

208 We trained an imputation model for each of the four AD-NC traits using 57
209 clinical variables obtained in MAP participants at the last visit before death as
210 predictors, by using the generalized linear regression model with Elastic-Net penalty
211 (GLM-EN) [45] (**Fig 1A**). Only MAP decedents with autopsy were used for developing
212 imputation models, because profiled AD-NC traits were required. By using the GLM-EN

213 method, variable selection was implemented and potential collinearity among clinical
214 variables was accounted for during model training. Since the Elastic-Net penalty is a
215 linear combination of L1 (i.e. LASSO) [46] and L2 (i.e., Ridge) [47] penalties on the
216 coefficients of clinical variables, variable selection are handled by the L1 penalty (i.e.,
217 penalizing the L1 norm of the coefficient vector) while potential collinearity is accounted
218 for by the L2 penalty (i.e., penalizing the L2 norm of the coefficient vector). Ten-fold
219 cross validation was used during model training to select Elastic-Net penalty parameters
220 (i.e., the proportions of L1 and L2 penalty) to ensure optimal imputation accuracy.

221 *Stage 2. Validating imputation models in a second independent cohort.*

222 Next, we validated the performance of the imputation models developed to infer
223 four AD-NC traits using clinical variables measured at the last visit proximate to death in
224 a second independent cohort with ROS decedents (**Fig 1A**). Prediction R^2 , the squared
225 correlation between inferred and measured values, was used for assessing imputation
226 accuracy for continuous AD-NC traits. Prediction accuracy for the dichotomous
227 pathologic AD diagnosis was evaluated by the predicted area under curve (AUC) values
228 of receiver operating characteristic curve (ROC) [48].

229 *Stage 3. Infer AD-NC traits at study entry and test their effectiveness as AD biomarkers*

230 Once imputation models are trained and validated, they can be applied to any
231 living adult with the same clinical variables measured. So, to illustrate the use of these
232 imputation models, we applied these validated models to the clinical data obtained from
233 ROS participants at study entry (i.e., baseline that was on average of eight years before
234 death or last follow-up visit) to infer baseline AD-NC traits (**Fig 1B**). Scatter plots and
235 ROC curves were used to evaluate the consistency between inferred AD-NC traits at

236 baseline and the corresponding measured postmortem AD-NC traits profiled at autopsy
237 in ROS decedents. Then we examined the effectiveness of inferred AD-NC traits as
238 potential AD biomarkers through two complementary analyses, one for evaluating the
239 predictivity for incident ADD by Cox proportional hazard model (Stage 3A) and the other
240 one for evaluating the discrimination of postmortem pathologic AD (Stage 3B).

241 Stage 3A. We fitted Cox proportional hazard models using covariates of age,
242 sex, education, and a single inferred baseline AD-NC trait in MAP cohort for predicting
243 incident ADD. Then we evaluated the performance of the Cox models for predicting
244 incident ADD in year 3 and year 5 from baseline in ROS cohort (**Fig S4**). Our fitted Cox
245 proportional hazard risk prediction models [49-51] also accounted for the competing risk
246 of death. The annual cognitive status diagnosis and the follow up year were used to
247 identify the first occurrence of ADD. For each participant, the year of enrollment is
248 considered as baseline (time 0), the year of first diagnosis of ADD is considered as the
249 time when the event occurs (incident ADD), and the last visit of participants without the
250 considered event during all follow-ups is considered as the right censored time for living
251 participants or the time of death for dead participants without ADD. Sample size
252 distributions with respect to cognitive status at baseline and the cognition event types
253 are shown in **Tables S1**. All Cox models were trained using data from MAP participants
254 (both living and deceased) and tested with data from ROS participants (both living and
255 deceased).

256 For fitting and testing Cox models for predicting incident ADD, we first used all
257 individuals without dementia at baseline, and then fitted and tested another set of Cox
258 models by using only individuals with NCI at baseline. For each set of Cox models fitted

259 by using MAP participants, we calculated model accuracy (AUC) for predicting incident
260 ADD in year 3 and year 5 from baseline.

261 Since Cox models provide a continuous risk score for incident ADD, by selecting
262 a risk score threshold corresponding to ~80% specificity (the proportion of correctly
263 predicted non-ADD in test ROS participant's, i.e., $1 - \text{false positive fraction}$), we could
264 calculate sensitivity (the proportion of true positive predictions in all test cases, i.e., true
265 positive fraction), and the overall classification accuracy (the proportion of true
266 discrimination of ADD in all test samples). Samples with risk scores greater than the
267 selected threshold were considered to develop ADD and less than the threshold as not
268 developing ADD in a specific year. That is, given the known ADD status of participants
269 in year 3 and year 5 from baseline, we can compare the predicted risk of incident ADD
270 to the actual incident ADD status to calculate the overall classification accuracy,
271 specificity, and sensitivity. Also, the sensitivity and specificity corresponding to a
272 selected risk score threshold reflect risk model performance at one point in the ROC
273 plots.

274 We also sequentially added the other three inferred baseline AD-NC traits into
275 the Cox model, in addition of covariates of age, sex, education, and inferred baseline
276 amyloid- β , and examined the prediction performance of these models.

277 Stage 3B. We examined the discrimination of inferred baseline levels of AD-NC
278 traits with respect to postmortem pathologic AD diagnosis (**Fig 1B**). Boxplots and two-
279 sample t-tests were used to evaluate the discrimination of postmortem pathologic AD by
280 inferred baseline AD-NC traits. Only ROS decedents with profiled pathologic AD
281 diagnoses were use in this discrimination analysis.

282

283 **RESULTS**

284 **Developed Imputation Models for Inferring AD-NC Traits**

285 Imputation models were trained to infer AD-NC traits by applying the GLM-EN
286 method using clinical measures in MAP decedents at their last visit before death as
287 predictors. Selected predictive clinical measures with standardized effect sizes
288 $|\beta| > 0.01$ estimated by the imputation models are shown in **Fig 2**. Composite
289 cognition score and *APOE E4* allele were the strongest predictors that were selected for
290 all four AD-NC traits. Yet, **Fig 2** also illustrates that varied non-cognitive clinical
291 measures including motor function such as motor gait and dexterity, health conditions
292 such as anxiety and hypertension, and medications such as lipid lowering and anti-
293 inflammatory medications were also selected. The effect size for motor gait was nearly
294 as strong as *APOE* for tangles, amyloid-beta, and global AD pathology.

295 These estimated effect sizes of selected clinical measure predictors in the
296 imputation models are used as weights to construct weighted sum with clinical
297 measurements to infer AD-NC trait levels. So, while all four AD-NC traits are related and
298 may share composite cognition score and *APOE E4* allele as important predictors, the
299 different sets of selected predictors by these four imputation models highlight that
300 mathematically different combinations of clinical measures with different estimated
301 effect sizes are necessary to best capture unique features of these inter-related AD-NC
302 traits.

303

304 **Validation of Imputation Models for Inferring AD-NC Traits**

305 To validate the imputation models developed in MAP decedents, we applied the
306 imputation models to clinical measures obtained at the last visit prior to death for
307 decedents in a second independent ROS cohort to infer their levels of four AD-NC traits.
308 Scatter plots illustrate the correlations between the inferred levels of the three
309 continuous AD-NC traits and their corresponding indices measured at autopsy (**Fig S5,**
310 **A-C**). The prediction R^2 was 0.188 for amyloid- β , 0.316 for tangles, and 0.262 for global
311 AD pathology (**Table S8**). An ROC plot (with AUC=0.765) illustrates the consistency
312 between the inferred probabilities of pathologic AD based on clinical measures obtained
313 at last visit before death versus the profiled pathologic AD status by autopsy (**Fig S5D;**
314 **Table S8**). As would be expected for effective AD biomarkers, all four inferred AD-NC
315 traits discriminated profiled pathologic AD at autopsy, with two-sample test P values <
316 10^{-28} (Box plots in **Fig S5; Table S8**). Together these results in a second independent
317 cohort validated the accuracy of the imputation models developed in MAP for all four
318 AD-NC traits.

319

320 **Inferred Baseline AD-NC Traits Predicted Incident ADD**

321 The imputation models were developed and validated using clinical measures at
322 the last visit prior to death in MAP and ROS decedents. In further analyses we
323 examined the effectiveness of inferred baseline AD-NC traits at study entry as AD
324 biomarkers. To infer baseline levels of four AD-NC traits at study entry, we applied the
325 validated imputation models to clinical data collected at baseline in all ROS participants
326 (n=1103; both living and decedents), an average of 8 years before death for decedents

327 (or last follow-up for living participants) (**Fig 1B**). Scatter plots of the three continuous
328 AD-NC traits and an ROC plot of the binary pathologic AD illustrate the correlation
329 between the inferred baseline versus the profiled AD-NC traits by autopsy (**Fig S6**).
330 Although the correlations were lower than the inferred AD-NC traits at last visit before
331 death (**Fig S5**), the following analyses with Cox models still demonstrated the
332 predictivity of the inferred baseline AD-NC traits for predicting incident ADD.

333 We employed separate Cox models that considered covariates age, sex,
334 education, and each one of the four inferred baseline AD-NC traits to examine the
335 predictivity for incident ADD (**Fig 3**). Coefficient estimates of the inferred baseline AD-
336 NC traits in these Cox models were provided along with the corresponding p-values in
337 **Table S9**. All inferred baseline AD-NC traits were strongly associated with incident
338 ADD, with p-values $< 10^{-30}$ in Cox models predicting incident ADD for adults without
339 dementia at baseline, and p-values $< 10^{-5}$ in Cox models for predicting incident ADD
340 from adults with NCI at baseline.

341 For all four AD-NC traits, model performance was higher in Year 3 (AUC ranging
342 in 0.861 – 0.919) versus Year 5 (AUC ranging in 0.842 – 0.896) from baseline (**Fig 3**,
343 **Upper Row**), for predicting incident ADD for adults without dementia at baseline. Of the
344 four AD-NC traits, inferred baseline probabilities of pathologic AD had the highest
345 predictivity (AUC 0.919 in Year 3; AUC 0.896 in Year 5) for incident ADD from adults
346 without dementia at baseline. Similar results were observed when we restricted the
347 analyses to the prediction of incident ADD in individuals with NCI at baseline (**Fig 3**,
348 **Lower Row**).

349 By selecting a risk score threshold corresponding the ~80% specificity, we
350 calculated sensitivity and accuracy based on the prediction results for all of the Cox
351 models (**Table 1**). Inferred baseline probabilities of pathologic AD also had the highest
352 accuracy rates (80%) and sensitivity for predicting incident ADD in Year 3 (0.911) and
353 Year 5 (0.829) from baseline (**Table 1**), compared to the other AD-NC traits.

354 In further analyses, we examined if adding covariates of additional inferred
355 baseline AD-NC traits in a single Cox model would improve the prediction accuracy for
356 incident ADD. As shown in **Fig S7 (Upper Row)**, we observed slightly improved AUC
357 for prediction of incident ADD in adults without dementia, when we sequentially added
358 each of the four AD-NC traits. Yet, modeling all four AD-NC traits together did not yield
359 better results than using inferred probabilities of pathologic AD alone (**Last Column of**
360 **Fig3 versus Fig S7**).

361 Sequentially adding the inferred baseline levels of three continuous AD-NC traits
362 (amyloid- β , tangles, and global AD pathology) in a single Cox model did not improve the
363 prediction of incident ADD for adults with baseline NCI (**Fig S7, Lower Row**). Although
364 adding the inferred baseline levels of the probabilities of pathologic AD improved the
365 prediction accuracy of incident ADD for adults with baseline NCI, but the prediction
366 accuracy was comparable as using the inferred baseline levels of the probabilities of
367 pathologic AD alone (**Last Column of Fig3 versus Fig S7**).

368

369 **Inferred Baseline AD-NC Traits Discriminated Postmortem Pathologic AD**

370 By examining if the inferred baseline AD-NC traits would discriminate
371 postmortem pathologic AD diagnosis, we presented boxplots of the inferred baseline

372 AD-NC traits of ROS decedents with respect to their postmortem pathologic AD
373 diagnosis by autopsy in **Fig 4**. By two-sample t-tests, we showed that all four inferred
374 baseline AD-NC traits discriminated individuals with postmortem pathologic AD
375 diagnosis by autopsy, with significant p-values $< 1.4 \times 10^{-10}$.

376

377 **DISCUSSION**

378 This study applied the machine learning GLM-EN methods to clinical
379 measurements and postmortem indices of four AD-NC traits (amyloid- β , tangles, global
380 AD pathology, and pathologic AD) obtained from the same older adults to develop
381 imputation models that could be used to infer levels of four AD-NC traits based on
382 clinical measurements. We validated these imputation models of AD-NC traits in a
383 second independent cohort of older adults that collected similar clinical and postmortem
384 indices. We applied the validated imputation models to clinical measures obtained at
385 study entry to infer baseline AD-NC traits in adults about an average of eight years
386 before death (decedents) or their last follow-up visit (living participants).

387 Adults without dementia at study entry who had higher baseline levels of inferred
388 AD-NC traits had a higher risk of developing incident ADD during follow-up years and
389 they also had a higher risk of having postmortem pathologic AD. These data suggest
390 that inferred levels of AD-NC traits based on clinical measures may provide a low cost,
391 non-invasive effective AD biomarker that can estimate the burden of AD-NC traits
392 during the chronic course of Alzheimer's disease. Inferred AD-NC traits may provide a
393 way to monitor the clinical course of the accumulation of AD-NC traits underlying
394 Alzheimer's disease, improve the homogeneity of clinical trials and catalyze early

395 targeted treatments to prevent the development of ADD in aging adults. Further studies
396 to validate longitudinal inferred AD-NC traits will be needed.

397

398 **Novelty of this Study**

399 Currently AD-NC traits in brain can only be measured at autopsy. Recent work has
400 focused on identifying effective AD biomarkers that can be used to assess levels of AD-
401 NC traits in living adults, especially during early stages of AD when cognition is still normal.
402 There are many prior studies that have examined the associations of clinical measures,
403 such as *APOE E4* allele, age, and cognitive measures, with future cognitive status or with
404 different AD/ADRD indices measured at autopsy including the postmortem diagnosis of
405 pathologic AD. Yet, it is important to note that the aim of these prior studies was not to
406 infer levels of the different AD-NC traits examined in this study, nor to test their
407 effectiveness as AD biomarkers [52-56].

408 Brain imaging studies of AD-NC traits have tried to employ serial imaging or CSF
409 fluid biomarkers as proxies to obtain measures of AD-NC traits in brains to assess the
410 accumulation of amyloid- β and tangles in early stages of Alzheimer's disease [18-20].
411 Recent work that compared tau and amyloid PET brain imaging to AD indices measured
412 at autopsy, suggests that current imaging may not reliably detect the early stages of AD
413 pathology [21, 22]. Yet, the expense and limited availability of brain imaging and the
414 invasiveness of obtaining CSF biomarkers make them difficult to be deployed at scale for
415 the general population. This study fills this gap by employing machine learning methods
416 that could be used to mathematically infer an AD-NC trait like "tangles" and estimate its
417 burden at any time point prior to death in any adult with the requisite clinical measures.

418 Obtaining structured autopsy and diverse clinical measures during annual follow-
419 ups, especially within a year prior of death, in large numbers of older adults is difficult.
420 Thus, it is novel to have two large cohorts like MAP or ROS with the same clinical and
421 postmortem indices of AD-NC traits that can be leveraged to develop imputation models
422 in one cohort and validate these imputation models in a second independent sample of
423 older adults. The rarity of these resources may explain in part the paucity of previous
424 studies trying to infer AD-NC traits based on clinical measurements alone.

425 Another novel feature of this study is that we provide evidence that inferred
426 baseline AD-NC traits on average 8 years before death for decedents (or before last visit
427 for living participants) may be used as effective AD biomarkers as they predicted incident
428 ADD and discriminated postmortem pathologic AD. That is, this study provides novel data
429 demonstrating the feasibility and effectiveness of developing imputation models to infer
430 AD-NC traits from clinical measures alone.

431

432 **Implications and Future Directions**

433 This study is best conceptualized as an important first step highlighting that new
434 machine learning analytic techniques can be used to infer AD-NC traits based on
435 clinical measures collected in older adults. Further studies are still needed to determine
436 if repeated inferred levels of AD-NC traits inform on trajectories of the accumulation of
437 these different AD-NC traits. Currently, the temporal course of accumulation of these
438 different AD-NC traits and the onset of their associations with impaired cognition are
439 unknown. Such data are crucial to determine if inferred AD-NC traits could be used to
440 assess the ongoing clinical course of Alzheimer's disease, and to assess the efficacy of

441 guiding treatments targeting specific AD-NC traits. For example, separate therapies
442 have been under study for targeting the peptide amyloid- β in extracellular amyloid
443 plaques and the protein tau in intracellular neurofibrillary tangles [7-9].

444 The analytic approach implemented in this study might also be extended to infer
445 the presence of other pathologies that are hard to measure in living adults and untangle
446 the effects of mixed-brain pathologies underlying late-life cognitive impairment and
447 dementia. Since many older adults with ADD show mixed-brain pathologies [57], further
448 work will be needed to develop analytic approaches that can infer and account for the
449 presence of different combinations of varied AD/ADRD pathologies.

450 Brain imaging as well as serum or fluid biomarkers were not examined in this
451 study, which could be used to validate the inferred levels of AD-NC traits by using our
452 developed imputation models. Additionally, the brain imaging and fluid biomarkers might
453 be included as additional predictors to enhance the imputation accuracy of AD-NC
454 traits, which could be crucial for untangling the relative contributions of mixed-brain
455 pathologies driving ADD in aging adults.

456

457 **Limitations and Strengths of this Study**

458 This study still has several limitations. First, participants were predominantly
459 Americans of European descent and have higher than average levels of education, so
460 our findings will need to be replicated in more diverse populations. Second, the current
461 study used diverse clinical predictors, many of that might not be available outside the
462 research setting such as the composite cognition score based on 19 cognitive tests
463 designed for ROS/MAP studies. Further work is needed to identify a parsimonious set of

464 clinical predictors that are more widely available to enhance the use of this approach in
465 diverse populations and geographic locations. Despite these limitations, this study is
466 best conceptualized as an important first step highlighting the potential of using machine
467 learning methods to infer AD-NC traits or other AD/ADRD pathologies based on clinical
468 measures that can be collected via remote phenotyping or electronic health records.

469 Nonetheless, this study has several strengths that lend confidence for the current
470 findings. All subjects were recruited from the community, underwent an annual detailed
471 clinical evaluation, and were without dementia based on their clinical assessment at
472 study entry. Large numbers of men and women underwent annual assessments, and
473 follow-up rates were very high (~90%) with an average of 8 years follow up. Uniform
474 and structured procedures were employed for the collection of clinical measures and
475 postmortem AD-NC traits in both MAP and ROS cohorts. An important strength of the
476 current study design is that we developed imputation models in MAP cohorts, and then
477 evaluated model performance in the second independent ROS cohort that employed
478 similar staff and data collection procedures [58].

479

480

481 **ACKNOWLEDGEMENTS**

482 We are deeply indebted to all participants who contributed their data and agreed to
483 autopsy at the time of their death. We thank the Rush Alzheimer's Disease Center staff
484 for their efforts.

485

486 **FUNDING**

487 This work was supported by the National Institute of Health R35GM138313,
488 P30AG10161, P30AG72975, K01AG054700, R01AG15819, R01AG17917,
489 R01AG56352; R01AG79133, the Illinois Department of Public Health; and the Robert C.
490 Borwell Endowment Fund. The funding organizations had no role in the design or
491 conduct of the study; collection, management, analysis, or interpretation of the data; or
492 preparation, review, or approval of the manuscript.

493

494 **CONFLICT OF INTEREST**

495 Jingjing Yang is an Editorial Board Member of this journal, but was not involved in the
496 peer-review process nor had access to any information regarding its peer-review. There
497 are no other disclosures nor conflict of interest for any of the authors.

498

499 **CONSENT STATEMENT**

500 Both MAP and ROS studies were approved by an Institutional Review Board of Rush
501 University Medical Center. All participants agreed to annual clinical evaluations and

502 autopsy at the time of death. Written informed consent was obtained from all study
503 participants as was an Anatomical Gift Act for organ donation.

504

505 **DATA AVAILABILITY**

506 All data analyzed in this study are de-identified and available to any qualified
507 investigator by submitting a request through the Rush Alzheimer's Disease Center
508 Research Resource Sharing Hub, <https://www.radc.rush.edu>, which has descriptions of
509 the studies and available data.

510

511 REFERENCES

- 512 [1] Hyman BT, Phelps CH, Beach TG, Bigio EH, Cairns NJ, Carrillo MC, Dickson DW,
513 Duyckaerts C, Frosch MP, Masliah E, Mirra SS, Nelson PT, Schneider JA, Thal DR, Thies B,
514 Trojanowski JQ, Vinters HV, Montine TJ (2012) National Institute on Aging–Alzheimer's
515 Association guidelines for the neuropathologic assessment of Alzheimer's disease.
516 *Alzheimer's and Dementia* **8**, 1-13.
- 517 [2] Ballard C, Gauthier S, Corbett A, Brayne C, Aarsland D, Jones E (2011) Alzheimer's
518 disease. *Lancet* **377**, 1019-1031.
- 519 [3] Jack CR, Jr., Albert M, Knopman DS, McKhann GM, Sperling RA, Carrillo MC, Thies B,
520 Phelps CH (2011) Introduction to revised criteria for the diagnosis of Alzheimer's
521 disease: National Institute on Aging and the Alzheimer's Association workgroup.
522 *Alzheimers Dement* **7**, 256-262.
- 523 [4] Wilson RS, Wang T, Yu L, Bennett DA, Boyle PA (2020) Normative Cognitive Decline in
524 Old Age. *Ann Neurol* **87**, 816-829.
- 525 [5] Boyle PA, Yu L, Leurgans SE, Wilson RS, Brookmeyer R, Schneider JA, Bennett DA (2019)
526 Attributable risk of Alzheimer's dementia attributed to age-related neuropathologies.
527 *Ann Neurol* **85**, 114-124.
- 528 [6] Yu L, Wang T, Wilson RS, Leurgans S, Schneider JA, Bennett DA, Boyle PA (2019)
529 Common age-related neuropathologies and yearly variability in cognition. *Ann Clin*
530 *Transl Neurol* **6**, 2140-2149.
- 531 [7] Zhang Y, Chen H, Li R, Sterling K, Song W (2023) Amyloid beta-based therapy for
532 Alzheimer's disease: challenges, successes and future. *Signal Transduct Target Ther* **8**,
533 248.
- 534 [8] Gotz J, Ittner A, Ittner LM (2012) Tau-targeted treatment strategies in Alzheimer's
535 disease. *Br J Pharmacol* **165**, 1246-1259.
- 536 [9] Lee HE, Lim D, Lee JY, Lim SM, Pae AN (2019) Recent tau-targeted clinical strategies for
537 the treatment of Alzheimer's disease. *Future Med Chem* **11**, 1845-1848.
- 538 [10] Lan MJ, Ogden RT, Kumar D, Stern Y, Parsey RV, Pelton GH, Rubin-Falcone H, Pradhaban
539 G, Zanderigo F, Miller JM, Mann JJ, Devanand DP (2017) Utility of Molecular and
540 Structural Brain Imaging to Predict Progression from Mild Cognitive Impairment to
541 Dementia. *J Alzheimers Dis* **60**, 939-947.
- 542 [11] Lu M, Pontecorvo MJ, Devous MD, Sr., Arora AK, Galante N, McGeehan A, Devadanam C,
543 Salloway SP, Doraiswamy PM, Curtis C, Trucchio SP, Flitter M, Locascio T, Devine M,
544 Zimmer JA, Fleisher AS, Mintun MA (2021) Aggregated Tau Measured by Visual
545 Interpretation of Flortaucipir Positron Emission Tomography and the Associated Risk of
546 Clinical Progression of Mild Cognitive Impairment and Alzheimer Disease: Results From 2
547 Phase III Clinical Trials. *JAMA Neurol* **78**, 445-453.
- 548 [12] Skillbäck T, Kornhuber J, Blennow K, Zetterberg H, Lewczuk P (2019) Erlangen Score
549 Predicts Cognitive and Neuroimaging Progression in Mild Cognitive Impairment Stage of
550 Alzheimer's Disease. *J Alzheimers Dis* **69**, 551-559.
- 551 [13] Janelidze S, Mattsson N, Palmqvist S, Smith R, Beach TG, Serrano GE, Chai X, Proctor NK,
552 Eichenlaub U, Zetterberg H, Blennow K, Reiman EM, Stomrud E, Dage JL, Hansson O
553 (2020) Plasma P-tau181 in Alzheimer's disease: relationship to other biomarkers,

- 554 differential diagnosis, neuropathology and longitudinal progression to Alzheimer's
555 dementia. *Nat Med* **26**, 379-386.
- 556 [14] Ansari A, Maffioletti E, Milanese E, Marizzoni M, Frisoni GB, Blin O, Richardson JC, Bordet
557 R, Forloni G, Gennarelli M, Bocchio-Chiavetto L (2019) miR-146a and miR-181a are
558 involved in the progression of mild cognitive impairment to Alzheimer's disease.
559 *Neurobiol Aging* **82**, 102-109.
- 560 [15] Faura J, Bustamante A, Penalba A, Giralt D, Simats A, Martínez-Sáez E, Alcolea D, Fortea
561 J, Lleó A, Teunissen CE, van der Flier WM, Ibañez L, Harari O, Cruchaga C, Hernández-
562 Guillamón M, Delgado P, Montaner J (2020) CCL23: A Chemokine Associated with
563 Progression from Mild Cognitive Impairment to Alzheimer's Disease. *J Alzheimers Dis* **73**,
564 1585-1595.
- 565 [16] Silbert LC, Howieson DB, Dodge H, Kaye JA (2009) Cognitive impairment risk: white
566 matter hyperintensity progression matters. *Neurology* **73**, 120-125.
- 567 [17] Greene SJ, Killiany RJ (2010) Subregions of the inferior parietal lobule are affected in the
568 progression to Alzheimer's disease. *Neurobiol Aging* **31**, 1304-1311.
- 569 [18] Braak H, Thal DR, Ghebremedhin E, Del Tredici K (2011) Stages of the pathologic process
570 in Alzheimer disease: age categories from 1 to 100 years. *J Neuropathol Exp Neurol* **70**,
571 960-969.
- 572 [19] Pettigrew C, Soldan A, Wang J, Wang MC, Greenberg B, Albert M, Moghekar A, Team BR
573 (2022) Longitudinal CSF Alzheimer's disease biomarker changes from middle age to late
574 adulthood. *Alzheimers Dement (Amst)* **14**, e12374.
- 575 [20] Johnson KA, Fox NC, Sperling RA, Klunk WE (2012) Brain imaging in Alzheimer disease.
576 *Cold Spring Harb Perspect Med* **2**, a006213.
- 577 [21] Ghirelli A, Tosakulwong N, Weigand SD, Clark HM, Ali F, Botha H, Duffy JR, Utianski RL,
578 Buciu M, Murray ME, Labuzan SA, Spsychalla AJ, Pham NTT, Schwarz CG, Senjem ML,
579 Machulda MM, Baker M, Rademakers R, Filippi M, Jack CR, Jr., Lowe VJ, Parisi JE,
580 Dickson DW, Josephs KA, Whitwell JL (2020) Sensitivity-Specificity of Tau and Amyloid β
581 Positron Emission Tomography in Frontotemporal Lobar Degeneration. *Ann Neurol* **88**,
582 1009-1022.
- 583 [22] Soleimani-Meigooni DN, Iaccarino L, La Joie R, Baker S, Bourakova V, Boxer AL, Edwards
584 L, Eser R, Gorno-Tempini ML, Jagust WJ, Janabi M, Kramer JH, Lesman-Segev OH,
585 Mellinger T, Miller BL, Pham J, Rosen HJ, Spina S, Seeley WW, Strom A, Grinberg LT,
586 Rabinovici GD (2020) 18F-flortaucipir PET to autopsy comparisons in Alzheimer's disease
587 and other neurodegenerative diseases. *Brain* **143**, 3477-3494.
- 588 [23] Jack CR, Jr., Holtzman DM (2013) Biomarker modeling of Alzheimer's disease. *Neuron*
589 **80**, 1347-1358.
- 590 [24] Darst BF, Lu Q, Johnson SC, Engelman CD (2019) Integrated analysis of genomics,
591 longitudinal metabolomics, and Alzheimer's risk factors among 1,111 cohort
592 participants. *Genet Epidemiol* **43**, 657-674.
- 593 [25] Chételat G, Arbizu J, Barthel H, Garibotto V, Law I, Morbelli S, van de Giessen E, Agosta
594 F, Barkhof F, Brooks DJ, Carrillo MC, Dubois B, Fjell AM, Frisoni GB, Hansson O, Herholz
595 K, Hutton BF, Jack CR, Jr., Lammertsma AA, Landau SM, Minoshima S, Nobili F, Nordberg
596 A, Ossenkoppele R, Oyen WJG, Perani D, Rabinovici GD, Scheltens P, Villemagne VL,

- 597 Zetterberg H, Drzezga A (2020) Amyloid-PET and (18)F-FDG-PET in the diagnostic
598 investigation of Alzheimer's disease and other dementias. *Lancet Neurol* **19**, 951-962.
- 599 [26] Isaacs JD, Boenink M (2020) Biomarkers for dementia: too soon for routine clinical use.
600 *Lancet Neurol* **19**, 884-885.
- 601 [27] Bălașa AF, Chircov C, Grumezescu AM (2020) Body Fluid Biomarkers for Alzheimer's
602 Disease-An Up-To-Date Overview. *Biomedicines* **8**, 421.
- 603 [28] Hastie T, Tibshirani R, Friedman J (2009) The elements of statistical learning: prediction,
604 inference and data mining. *Springer-Verlag, New York*.
- 605 [29] Feng X, Chen L, Wang Z, Li SC (2020) I-Impute: a self-consistent method to impute single
606 cell RNA sequencing data. *BMC Genomics* **21**, 618.
- 607 [30] Li WV, Li JJ (2018) An accurate and robust imputation method scImpute for single-cell
608 RNA-seq data. *Nat Commun* **9**, 997.
- 609 [31] Gamazon ER, Wheeler HE, Shah KP, Mozaffari SV, Aquino-Michaels K, Carroll RJ, Eyster
610 AE, Denny JC, Nicolae DL, Cox NJ, Im HK (2015) A gene-based association method for
611 mapping traits using reference transcriptome data. *Nat Genet* **47**, 1091-1098.
- 612 [32] Nguyen M, He T, An L, Alexander DC, Feng J, Yeo BTT (2020) Predicting Alzheimer's
613 disease progression using deep recurrent neural networks. *Neuroimage* **222**, 117203.
- 614 [33] Nagpal S, Meng X, Epstein MP, Tsoi LC, Patrick M, Gibson G, De Jager PL, Bennett DA,
615 Wingo AP, Wingo TS, Yang J (2019) TIGAR: An Improved Bayesian Tool for
616 Transcriptomic Data Imputation Enhances Gene Mapping of Complex Traits. *Am J Hum*
617 *Genet* **105**, 258-266.
- 618 [34] Luningham JM, Chen J, Tang S, De Jager PL, Bennett DA, Buchman AS, Yang J (2020)
619 Bayesian Genome-wide TWAS Method to Leverage both cis- and trans-eQTL Information
620 through Summary Statistics. *Am J Hum Genet* **107**, 714-726.
- 621 [35] Bennett DA, Buchman AS, Boyle PA, Barnes LL, Wilson RS, Schneider JA (2018) Religious
622 Orders Study and Rush Memory and Aging Project. *J Alzheimers Dis* **64**, S161-S189.
- 623 [36] Bennett DA, Schneider JA, Wilson RS, Bienias JL, Arnold SE (2004) Neurofibrillary tangles
624 mediate the association of amyloid load with clinical Alzheimer disease and level of
625 cognitive function. *Arch Neurol* **61**, 378-384.
- 626 [37] Bennett DA, Wilson RS, Schneider JA, Evans DA, Aggarwal NT, Arnold SE, Cochran EJ,
627 Berry-Kravis E, Bienias JL (2003) Apolipoprotein E epsilon4 allele, AD pathology, and the
628 clinical expression of Alzheimer's disease. *Neurology* **60**, 246-252.
- 629 [38] Bennett DA, Wilson RS, Schneider JA, Evans DA, Mendes De Leon CF, Arnold SE, Barnes
630 LL, Bienias JL (2003) Education modifies the relation of AD pathology to level of
631 cognitive function in older persons. *Neurology* **60**, 1909-1915.
- 632 [39] Bennett DA, Wilson RS, Boyle PA, Buchman AS, Schneider JA (2012) Relation of
633 neuropathology to cognition in persons without cognitive impairment. *Ann Neurol* **72**,
634 599-609.
- 635 [40] (1997) Consensus recommendations for the postmortem diagnosis of Alzheimer's
636 disease. The National Institute on Aging, and Reagan Institute Working Group on
637 Diagnostic Criteria for the Neuropathological Assessment of Alzheimer's Disease.
638 *Neurobiol Aging* **18**, S1-2.

- 639 [41] Wilson RS, Boyle PA, Yu L, Barnes LL, Sytsma J, Buchman AS, Bennett DA, Schneider JA
640 (2015) Temporal course and pathologic basis of unawareness of memory loss in
641 dementia. *Neurology* **85**, 984-991.
- 642 [42] Boyle PA, Wilson RS, Aggarwal NT, Tang Y, Bennett DA (2006) Mild cognitive
643 impairment: risk of Alzheimer disease and rate of cognitive decline. *Neurology* **67**, 441-
644 445.
- 645 [43] McKhann GM, Knopman DS, Chertkow H, Hyman BT, Jack CR, Jr., Kawas CH, Klunk WE,
646 Koroshetz WJ, Manly JJ, Mayeux R, Mohs RC, Morris JC, Rossor MN, Scheltens P, Carillo
647 MC, Thies B, Weintraub S, Phelps CH (2011) The diagnosis of dementia due to
648 Alzheimer's disease: Recommendations from the National Institute on Aging and the
649 Alzheimer's Association workgroup. *Alzheimers Dement*.
- 650 [44] Bennett DA, Schneider JA, Arvanitakis Z, Kelly JF, Aggarwal NT, Shah RC, Wilson RS
651 (2006) Neuropathology of older persons without cognitive impairment from two
652 community-based studies. *Neurology* **66**, 1837-1844.
- 653 [45] Zou H, Hastie T (2005) Regularization and variable selection via the elastic net. *Journal of*
654 *the Royal Statistical Society: Series B (Statistical Methodology)* **67**, 301-320.
- 655 [46] Tibshirani R (1996) Regression Shrinkage and Selection via the Lasso. *Journal of the*
656 *Royal Statistical Society. Series B (Methodological)* **58**, 267-288.
- 657 [47] Hoerl AE, Kennard RW (2000) Ridge Regression: Biased Estimation for Nonorthogonal
658 Problems. *Technometrics* **42**, 80-86.
- 659 [48] Linden A (2006) Measuring diagnostic and predictive accuracy in disease management:
660 an introduction to receiver operating characteristic (ROC) analysis. *J Eval Clin Pract* **12**,
661 132-139.
- 662 [49] Cox DR (1972) Regression models and life-tables. *Journal of the Royal Statistical Society:*
663 *Series B (Methodological)* **34**, 187-202.
- 664 [50] Gerds TA, Scheike TH, Andersen PK (2012) Absolute risk regression for competing risks:
665 interpretation, link functions, and prediction. *Stat Med* **31**, 3921-3930.
- 666 [51] Ozenne B, Sørensen AL, Scheike T, Torp-Pedersen C, Gerds TA (2017) riskRegression:
667 predicting the risk of an event using Cox regression models. *The R Journal* **9**, 440-460.
- 668 [52] Powell MR, Smith GE, Knopman DS, Parisi JE, Boeve BF, Petersen RC, Ivnik RJ (2006)
669 Cognitive measures predict pathologic Alzheimer disease. *Arch Neurol* **63**, 865-868.
- 670 [53] Dickerson BC, Sperling RA, Hyman BT, Albert MS, Blacker D (2007) Clinical prediction of
671 Alzheimer disease dementia across the spectrum of mild cognitive impairment. *Arch*
672 *Gen Psychiatry* **64**, 1443-1450.
- 673 [54] Petersen RC, Smith GE, Ivnik RJ, Tangalos EG, Schaid DJ, Thibodeau SN, Kokmen E,
674 Waring SC, Kurland LT (1995) Apolipoprotein E status as a predictor of the development
675 of Alzheimer's disease in memory-impaired individuals. *JAMA* **273**, 1274-1278.
- 676 [55] Bondi MW, Salmon DP, Galasko D, Thomas RG, Thal LJ (1999) Neuropsychological
677 function and apolipoprotein E genotype in the preclinical detection of Alzheimer's
678 disease. *Psychol Aging* **14**, 295-303.
- 679 [56] Phongpreecha T, Cholerton B, Bukhari S, Chang AL, De Francesco D, Thuraiappah M,
680 Godrich D, Perna A, Becker MG, Ravindra NG, Espinosa C, Kim Y, Berson E, Mataraso S,
681 Sha SJ, Fox EJ, Montine KS, Baker LD, Craft S, White L, Poston KL, Beecham G,

- 682 Aghaeepour N, Montine TJ (2023) Prediction of neuropathologic lesions from clinical
683 data. *Alzheimers Dement* **19**, 3005-3018.
- 684 [57] Schneider JA, Arvanitakis Z, Bang W, Bennett DA (2007) Mixed brain pathologies account
685 for most dementia cases in community-dwelling older persons. *Neurology* **69**, 2197-
686 2204.
- 687 [58] Licher S, Yilmaz P, Leening MJG, Wolters FJ, Vernooij MW, Stephan BCM, Ikram MK,
688 Ikram MA (2018) External validation of four dementia prediction models for use in the
689 general community-dwelling population: a comparative analysis from the Rotterdam
690 Study. *Eur J Epidemiol* **33**, 645-655.
691

692 **Figure Legends**

693 **Fig 1. Overall study design to develop and validate imputation models that infer**
694 **AD-NC traits based on clinical measures in older adults.** A multi-stage analytic
695 approach was employed to develop, validate, and demonstrate the effectiveness of
696 inferred levels of four AD-NC traits derived from clinical measures as AD biomarkers. **A.**
697 We trained imputation models for four AD-NC traits using clinical data obtained at the last
698 visit before death in MAP decedents that underwent autopsy (**Fig 2**). Then we validated
699 these models in an independent cohort study (ROS) that collected the same clinical and
700 postmortem measures. **B.** We tested the effectiveness as AD biomarkers for the inferred
701 levels of four AD-NC traits at baseline, which were obtained by applying the validated
702 imputation models to clinical measures obtained at study entry. We examined if the
703 inferred baseline AD-NC traits predicted incident ADD (**Fig 3**) and discriminated adults at
704 risk for postmortem (on average 8 years after baseline) pathologic AD in ROS cohort (**Fig**
705 **4**).

706 **Fig 2. Machine learning methods were used to select different combinations of**
707 **clinical measures to infer each of the four AD-NC traits.** GLM-EN method was used
708 to train an imputation model for each of the four AD-NC traits. Standardized effect sizes
709 (beta) of selected predictive predictors with $|\text{beta}| > 0.01$ for each of the four imputation
710 models were plotted. The inferred values of each of the inferred AD-NC traits are
711 determined by the weighted averages of the corresponding selected predictors, with
712 weights given by estimated standard effect sizes. Although all four AD-NC traits are
713 inter-related and share cognition and *APOE E4* allele as important predictors, different
714 sets of selected predictors by their imputation models highlight that different
715 combinations of clinical measures with different effect sizes are necessary for inferring
716 the unique features of these inter-related AD-NC traits.

717
718 **Fig 3. Inferred baseline AD-NC traits predicted incident Alzheimer's Disease**
719 **Dementia (ADD).** We used Cox proportional hazard models to examine the predictivity
720 of each of the inferred baseline AD-NC traits along with age, sex, and education
721 covariates for incident ADD in 3 and 5 years after study entry. Top four panels show the
722 prediction accuracies (ROC plots) with each the four inferred baseline AD-NC traits in
723 adults without dementia (NCI+MCI) at study entry. Bottom four panels show prediction
724 accuracies with each of the four AD-NC traits in adults with NCI at study entry. As
725 expected for an effective AD biomarker, each of the inferred baseline AD-NC traits
726 predicted ADD.

727 **Fig 4. Inferred AD-NC traits at study baseline discriminated postmortem pathologic**
728 **AD profiled at autopsy.** Pathologic AD here is the binary postmortem NIA-Reagan status
729 profiled at autopsy, with value 1 representing pathologic AD (teal boxplots) and 0
730 representing no pathologic AD (red boxplots). Two-sample t-test p-values are 1.4×10^{-10}
731 for amyloid- β (A), 1.2×10^{-11} for tangles (B), 9.8×10^{-12} for global AD pathology (C), and
732 1.6×10^{-10} for pathologic AD (D).

733

Table 1. Prediction accuracy (with 95% confidence interval) and sensitivity with respect to selected risk score thresholds that ensure ~80% specificity by Cox models using a single inferred AD-NC trait. Values in this table are reflecting the Cox risk model prediction performance at one point in the ROC curves as shown in **Fig 3**, with corresponding risk score thresholds. Samples with predicted risk scores greater than the selected threshold were considered as Predicted Positives (incident ADD), otherwise Predicted Negatives (not developing ADD).

		Amyloid- β		Tangles		Global AD Pathology		Pathologic AD	
		Y3	Y5	Y3	Y5	Y3	Y5	Y3	Y5
NCI/MCI -> ADD	Accuracy^a (95% CI)	0.798 (0.773, 0.822)	0.788 (0.763, 0.813)	0.802 (0.777, 0.825)	0.795 (0.771, 0.818)	0.801 (0.775, 0.823)	0.796 (0.771, 0.819)	0.809 (0.784, 0.831)	0.803 (0.778, 0.826)
	Sensitivity^b	0.772	0.699	0.822	0.756	0.797	0.764	0.911	0.829
	Specificity^c	0.800	0.800	0.800	0.800	0.800	0.800	0.800	0.800
NCI -> ADD	Accuracy^a (95% CI)	0.796 (0.768, 0.823)	0.792 (0.763, 0.7819)	0.794 (0.765, 0.821)	0.791 (0.761, 0.818)	0.795 (0.767, 0.823)	0.793 (0.764, 0.820)	0.804 (0.775, 0.830)	0.805 (0.777, 0.832)
	Sensitivity^b	0.650	0.634	0.550	0.609	0.600	0.658	0.950	0.902
	Specificity^c	0.800	0.800	0.800	0.800	0.800	0.800	0.800	0.800

a. Accuracy= (# True Positive Predictions + # True Negative Predictions) / (# of test samples)

b. Sensitivity = (# True Positive Predictions) / (# Positives in test samples) = True Positive Fraction

c. Specificity = (# True Negative Predictions) / (# Negatives in test samples) = 1 – False Positive Fraction

FIGURES

Fig 1. Overall study design to develop and validate imputation models that infer AD-NC traits based on clinical measures in older adults. A multi-stage analytic approach was employed to develop, validate, and demonstrate the effectiveness of inferred levels of four AD-NC traits derived from clinical measures as AD biomarkers. **A.** We trained imputation models for four AD-NC traits using clinical data obtained at the last visit before death in MAP decedents that underwent autopsy (**Fig 2**). Then we validated these models in an independent cohort study (ROS) that collected the same clinical and postmortem measures. **B.** We tested the effectiveness as AD biomarkers for the inferred levels of four AD-NC traits at baseline, which were obtained by applying the validated imputation models to clinical measures obtained at study entry. We examined if the inferred baseline AD-NC traits predicted incident ADD (**Fig 3**) and discriminated adults at risk for postmortem (on average 8 years after baseline) pathologic AD in ROS cohort (**Fig 4**).

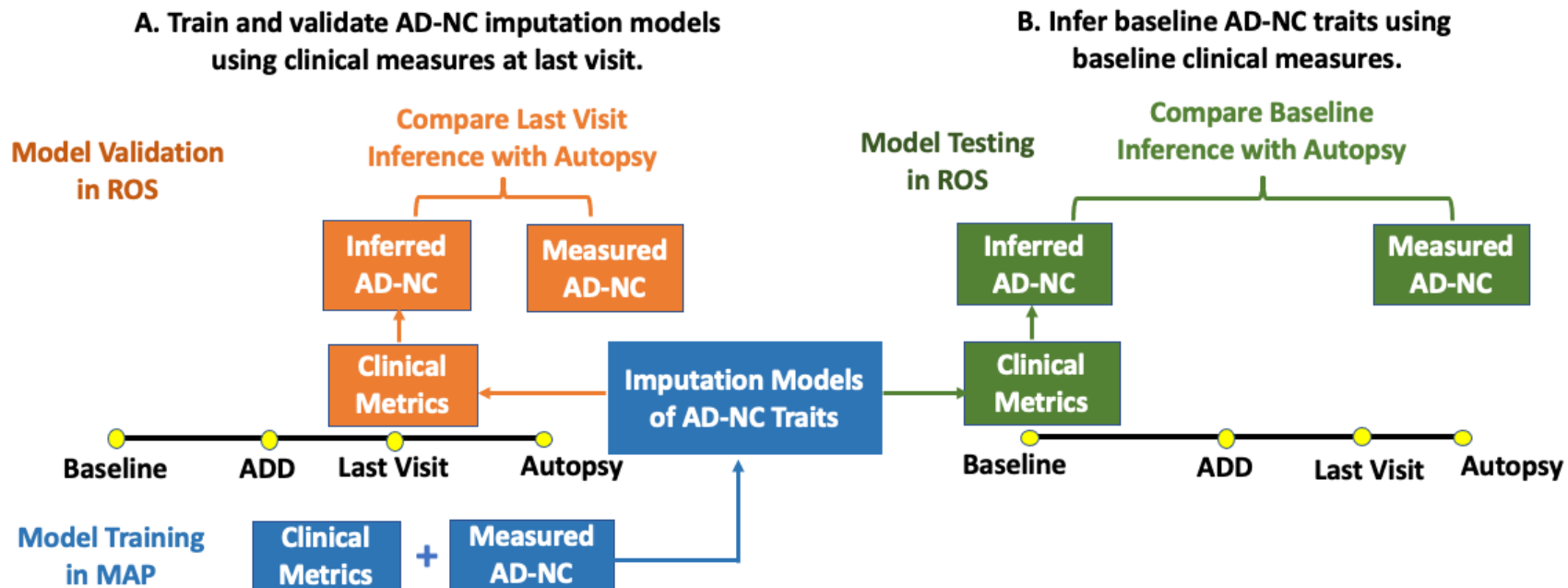


Fig 2. Machine learning methods were used to select different combinations of clinical measures to infer each of the four AD-NC traits. GLM-EN method was used to train an imputation model for each of the four AD-NC traits. Standardized effect sizes (beta) of selected predictive predictors with $|\text{beta}| > 0.01$ for each of the four imputation models were plotted. The inferred values of each of the inferred AD-NC traits are determined by the weighted averages of the corresponding selected predictors, with weights given by estimated standard effect sizes. Although all four AD-NC traits are inter-related and share cognition and *APOE E4* allele as important predictors, different sets of selected predictors by their imputation models highlight that different combinations of clinical measures with different effect sizes are necessary for inferring the unique features of these inter-related AD-NC traits.

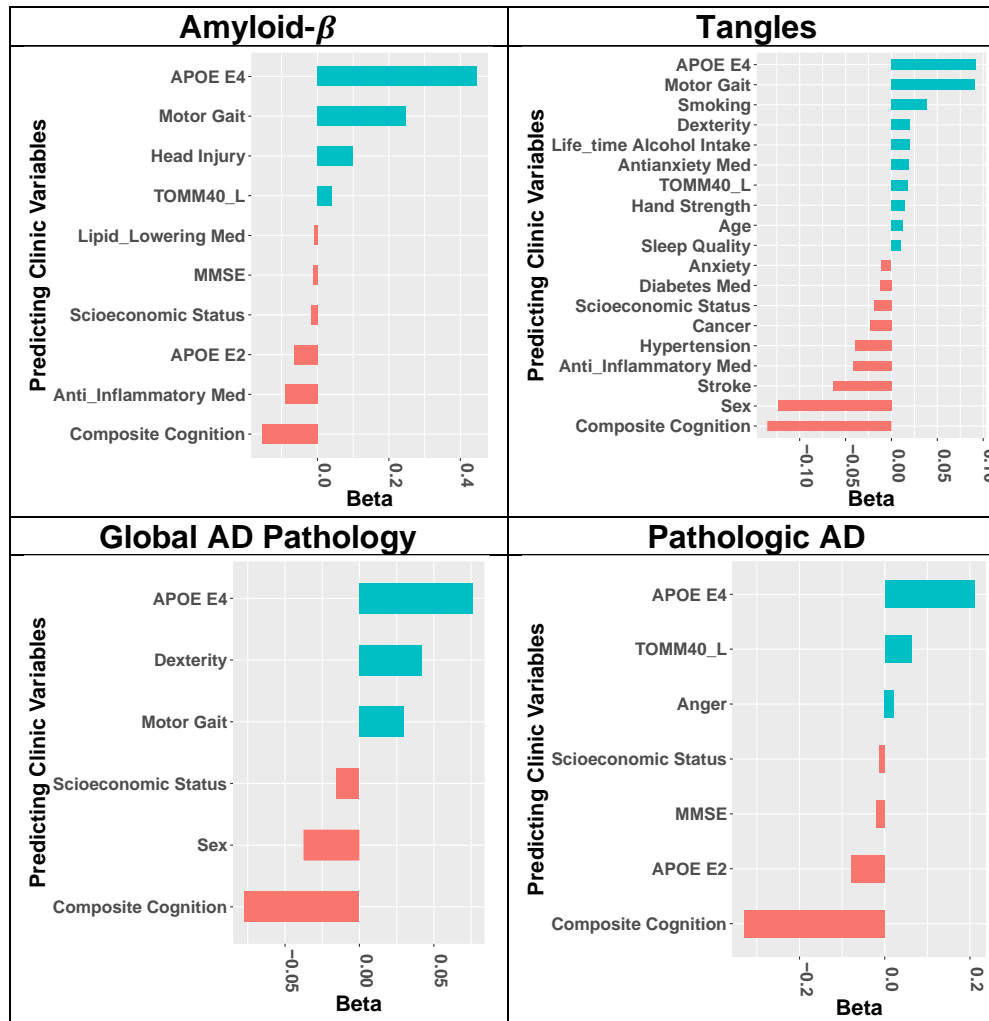


Fig 3. Inferred baseline AD-NC traits predicted incident Alzheimer’s Disease Dementia (ADD). We used Cox proportional hazard models to examine the predictivity of each of the inferred baseline AD-NC traits along with age, sex, and education covariates for incident ADD in 3 and 5 years after study entry. Top four panels show the prediction accuracies (ROC plots) with each the four inferred baseline AD-NC traits in adults without dementia (NCI+MCI) at study entry. Bottom four panels show prediction accuracies with each of the four AD-NC traits in adults with NCI at study entry. As expected for an effective AD biomarker, each of the inferred baseline AD-NC traits predicted ADD.

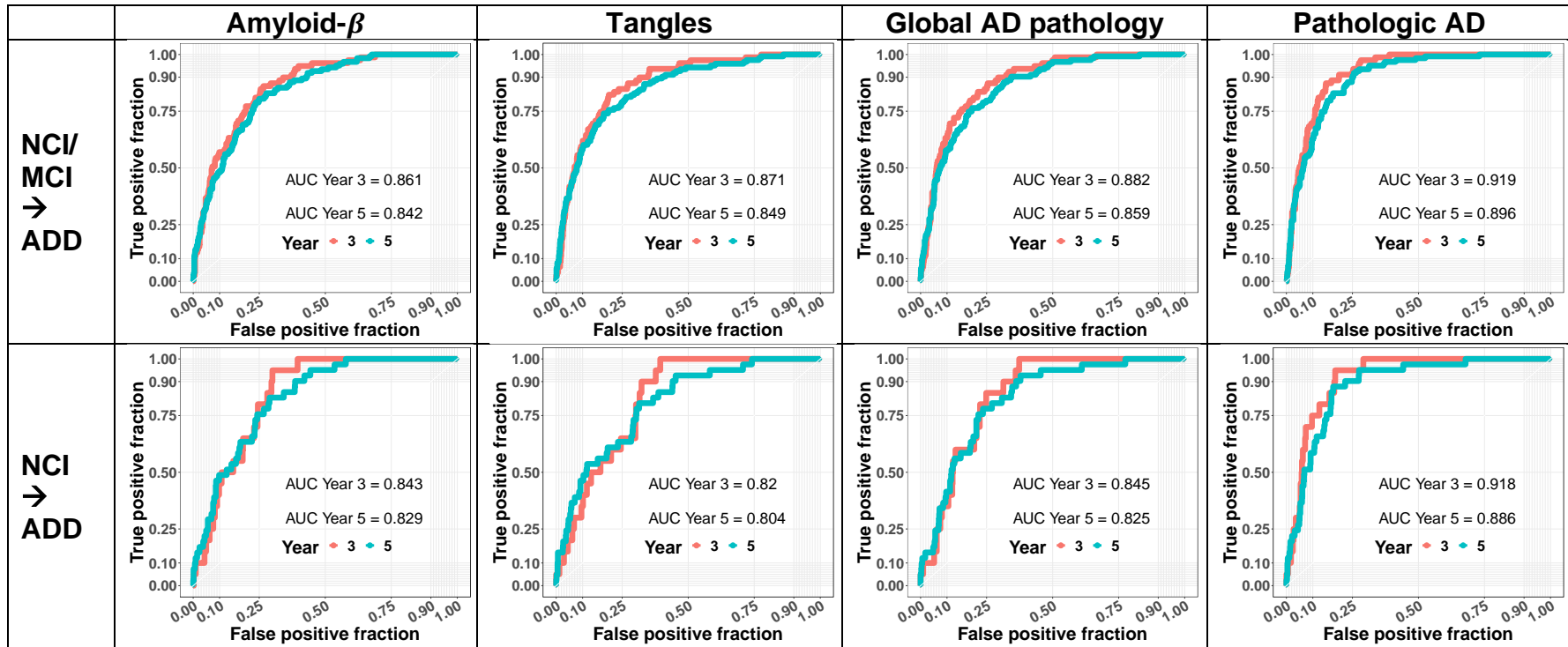


Fig 4. Inferred AD-NC traits at study baseline discriminated postmortem pathologic AD profiled at autopsy. Pathologic AD here is the binary postmortem NIA-Reagan status profiled at autopsy, with value 1 representing pathologic AD (teal boxplots) and 0 representing no pathologic AD (red boxplots). Two-sample t-test p-values are 1.4×10^{-10} for amyloid- β (A), 1.2×10^{-11} for tangles (B), 9.8×10^{-12} for global AD pathology (C), and 1.6×10^{-10} for pathologic AD (D).

